Single Crystalline Scandium Aluminum Nitride: An Emerging Material for 5G Acoustic Filters

Azadeh Ansari
School of Electrical and Computer Engineering, Georgia Institute of Technology, Atlanta, GA

***Abstract*—Emerging next generation wireless communication devices call for high-performance filters that operate at 3-10 GHz frequency range and offer low loss, small form factor, wide bandwidth and steep skirts. Bulk and surface acoustic wave devices have been long used in the RF front-end for filtering applications, however their operation frequencies are mostly below 2.6 GHz band. To scale up the frequency of the filters, the thickness of the piezoelectric material needs to be reduced to sub-micron ranges. One of the challenges of such scaling is maintaining high electromechanical coupling as the film thickness decreases, which in turn, determines the filter bandwidth.**

Aluminum Nitride (AlN) — popular in today's film bulk acoustic resonators (FBARs) and mostly deposited using sputtering techniques—shows degraded crystal quality and poor electromechanical coupling when the thickness of AlN film is smaller than 1 μm.

In this work, we propose using high-quality single-crystalline AlN and Scandium (Sc)-doped AlN epi-layers grown on Si substrates, wherein high crystal quality is maintained for ultra-thin films of only 400 nm thickness. Experimental results verify improved k_t^2 for 3-10 GHz resonators, with quality factors of the order of ~250 and k_t^2 values of up to 5%based on bulk acoustic wave resonators. The experimental results suggest that single-crystal Sc-AlN is a great material candidate for 5G resonators and filters.

***Index Terms*—5G mobile communication, Piezoelectric devices, Acoustic Filters, Wide band gap semiconductors, Single Crystalline, Scandium Doping, Aluminum Nitride.**

I. Introduction

Emerging 5G, and 4G LTE communication standards call for high performance filters that operate above 2.6 GHz and offer low loss, large bandwidth, and steep skirts in wireless communication devices [1]. This enquires high-performance acoustic resonators as building blocks in filters, that offer (1) large quality factor (Q) which determines the insertion loss of the filter, (2) high effective electromechanical coupling coefficient (k_t^2), which determines the bandwidth, (3) low temperature coefficient of frequency (TCF), which determines the filter frequency stability and (4) good power handling capability. The center frequencies of such devices should cover newer LTE frequency bands at 3.4-3.8 GHz [2], emerging 5G bands in 3.3-4.99 GHz [2], and higher 5G bands of 26 GHz range [3].

Bulk acoustic wave (BAW) and surface acoustic wave (SAW) filters have been widely used and known to satisfy the stringent criteria required for radio frequency communication. Traditionally, they have been optimized to target 100 MHz to 2.6 GHz. Different piezoelectric materials have been used for SAW and BAW applications with thicknesses ranging from 2 to 10 μm. Amongst them, AlN has been popular mainly due to CMOS compatibility, and well-developed micromachining techniques and relatively low temperature coefficient of frequency (TCF), which is less than a quarter of the TCF of $LiNbO_3$ [4]. However, AlN's moderate electromechanical coupling coefficient compared to $LiNbO_3$ devices is considered a major drawback [5].

Scandium-doping of aluminum nitride (ScAlN) has shown promising results in terms of higher piezoelectric coefficients. Enhanced piezoelectric effects directly influence the electromechanical coupling coefficient as shown in Eq. 1. Electromechanical coupling coefficient up to 4 times larger than pure AlN was reported due to enhanced piezo-response in Sc-doped AlN [6].

$$K^2 = \frac{c \cdot d_{33}^2}{\varepsilon_0 \varepsilon_r}, \qquad \text{(Eq. 1)}$$

where c is the effective elastic constant, d_{33} is the piezoelectric coefficient, ε_0 is vacuum permittivity and ε_r is the relative dielectric constant. Besides Sc-doping, the crystal quality of the piezoelectric material plays an important role in the performance of the acoustic filters [7].

The most common method for deposition of AlN and ScAlN is reactive magnetron sputtering [8]. Although this simple technique is attractive due to low cost and relatively high growth rates, crystal quality of the layers is inferior compared to those grown using epitaxial methods that use high vacuum conditions.

With bulky devices that target low to moderate frequencies (< 2.6 GHz), the effect of poly crystallinity can be averaged out. However, crystallinity becomes significant when the device thickness is scaled down to achieve higher frequency ranges. It is shown in [7] that the functional material properties of AlN improve with film thickness when increased from 35 nm to 2 μm. For example, Full Width at Half Maximum (FWHM) values were improved from 2.60° to 1.14° and the effective d_{33} piezoelectric coefficients, namely $d_{33,f}$, increased from 2.75 to 5.15 pm/V.

Overall, there is a strong correlation between the crystallinity of the device layer and the piezoelectric coefficients. The same effect has also been shown in gallium nitride (GaN) resonators and filters, which has the same Wurtzite crystal structure as AlN and ScAlN [9-10]. Since poly-crystalline film thickness and FWHM directly affect the electromechanical coupling coefficient and thus the bandwidth of the filter, it is crucial to grow sub-micron thin films that maintain high crystal quality and offer high electromechanical coupling.

In this paper, we introduce single crystalline Sc-AlN as an emerging material for acoustic devices for wireless communication. By taking advantage of high crystal quality of

AlN epi-layers, as well as the enhanced piezo-response due to Sc-doping, we report on high-performance resonators operating at 3-10 GHz that are the main building blocks of Acoustic filters.

Single crystalline AlN and ScAlN device layers were grown by molecular beam epitaxy (MBE) on silicon substrates by IQE plc [12] and used to build SAW and BAW resonators. While, metal organic chemical vapor deposition (MOCVD), widely used for growth of III-N layers for electronic and photonic devices, is used to grow AlN, it is not suitable for growth of ScAlN because of the absence of scandium precursors and the required separation of phases for reliable decomposition of the precursors at typical MOCVD process temperatures [13].

II. Material Growth And Fabrication Process

AlN and ScAlN (with a doping concentration of 12%) layers with thickness of 400 nm were grown using molecular beam epitaxy (MBE) by evaporation of pure metals from effusion cells using nitrogen plasma. Growth rate was 0.5 Å/s at substrate temperature of 1370 K and 970 K for AlN and ScAlN, respectively. High-resolution transmission electron microscopy (HRTEM) (Fig. 1(a)) and scanning electron microscope (SEM) (Fig. 1(b)) were used to analyze the crystal structures of the layers. X-ray diffraction (XRD) and omega scan showed a full width at half maximum (FWHM) of 1800 arcseconds and 4320 arcseconds for AlN and ScAlN layers, respectively (Fig. 1(c)-(e)). It must be taken into account that thickness of the layers is 400 nm, which is substantially lower compared to the thickness of the sputtered layers used by other groups, shown in Table I.

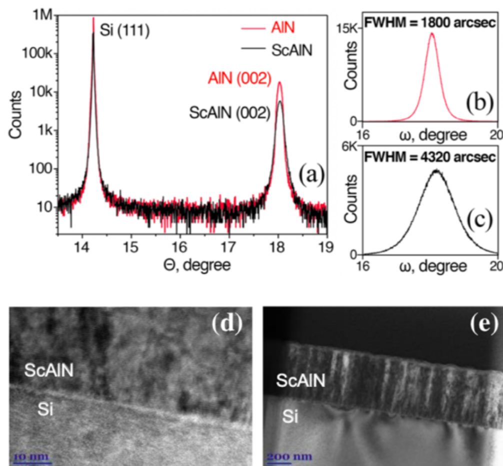

Fig. 1. (a) HRTEM and (b) SEM of ScAlN, and (c) XRD, and (d) omega scan of AlN and (e) ScAlN. Samples were grown by IQE plc [12].

To ensure high electromechanical coupling, the wavelength of the SAW and Lamb-wave devices were designed to be two times the thickness of the thin film (λ =800 nm) [14]. Each interdigitated transducer finger width is 200 nm and is defined with electron-beam lithography. The fabrication of SAW resonators and filters is a simple one-mask process. However, the fabrication process of Lamb-wave resonators requires plasma etching of AlN trenches and exposing the Si substrate to Xenon Difluride (XeF_2) isotropic etch. Fig. 2 summarizes the fabrication steps. Fig. 2 (a,b) depict the fabrication of a SAW resonator/filter and Fig. 2(c,d) show the fabrication process of a Lamb-wave resonator. The etching process of trenches using Oxide hard mask and the release step are demonstrated. Scanning Electron Microscope (SEM) images of the final device structures are shown in Fig. 3.

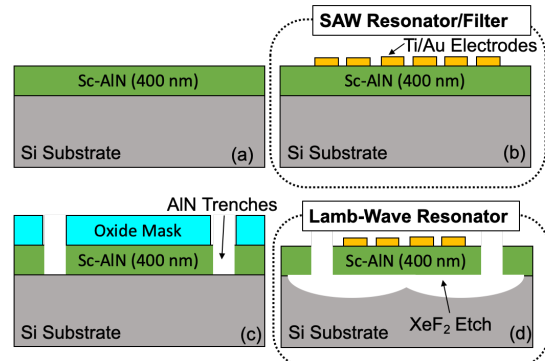

Fig. 2. (a) 400 nm AlN-on-Si starting epi-wafer. (b) Fabrication process of a one-step exposure of the SAW devices. (c) Patterning Oxide hard mask and etching AlN in a Cl_2-based plasma etch. (d) Isotropic etching of the Si substrate to relaese the membrane for Lamb wave resonators.

SAW delay lines can be directly fabricated based on AlN-on-Si substrates to build acoustic filters. Lamb-wave resonators can also form delay-line structures or similar to FBARs can be placed in ladder-type or lattice-type configurations as the building block of acoustic filters. The performance of such acoustic filters is determined by the electromechanical coupling (k_t^2), Q, series and parallel frequency (f_s and f_p) of the constituent resonator block.

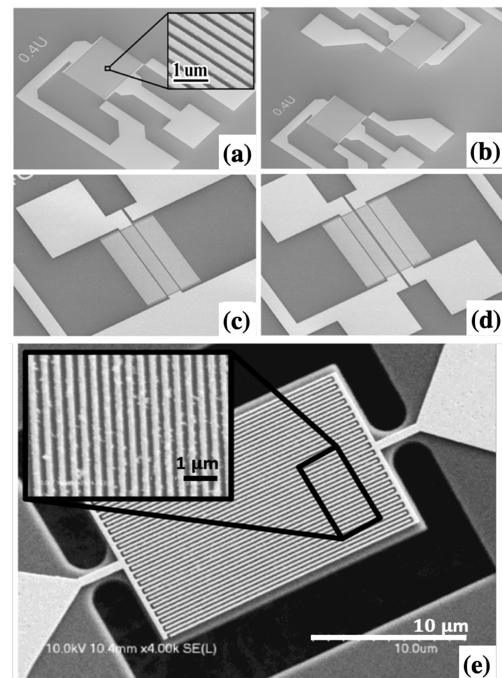

Fig. 3. SEM images of the fabricated devices of (a-d) SAW and (e) Lamb wave resonator. (a) one-port; (b) one-port with reflector; (c) two-port (d) two-port with reflectors SAW devices. (e) Lamb-wave resonator with bevelled tethers and trenches. Two electrode width variation of 300 nm and 400 nm were included in the layout. SEM images are taken from [15-16].

III. Experimental Results of Device Performance

Scattering matrix (S)-parameters were measured over the frequency range from 1 to 10 GHz for the SAW devices and 1-20 GHz for the Lamb-wave devices, the wide band response and corresponding zoomed-in peaks are shown in Fig. 4. Admittance (Y_{11})-parameter was used to determine parallel resonant frequency (f_p), series resonant frequency (f_s), and effective electromechanical coupling coefficient (k_t^2). Q was extracted from the MBVD model [17], and k_t^2[18] was extracted using Eq. 2:

$$k_t^2 = \frac{\pi^2}{4}\left(f_p - f_s\right)\frac{f_s}{f_p^2}. \quad \text{(Eq. 2)}$$

The measurement results of the SAW devices are compared against other SAW devices using sputter-deposited AlN in Table I, showing significant improvement of $Q \times k_t^2$ figure of merit.

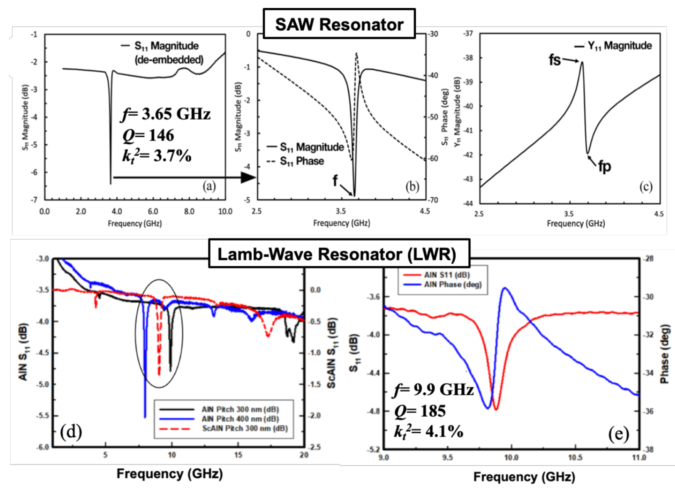

Fig. 4. (a-c) Measurement results ScAlN/Si SAW resonator: (a) 1-10 GHz de-embedded and (b) zoomed-in magnitude and phase; (c) Zoomed-in Y_{11} frequency response. (d-e) Lamb wave measurement results (d) S_{11} wide band frequency response of the Lamb-wave resonator shown in Fig. 3(e). (e) Zoomed-in resonance peak at 9.9 GHz.

Table I. Comparison with sputtered AlN/ScAlN devices on Si substrates.

Materials	Type	f (GHz)	Q	k_t^2 (%)	$Q \times k_t^2$
Sputtered Sc(27%) AlN/Si	SAW [11]	0.294	100	2.2	2.2
Single crystalline Sc(12%)AlN/Si	SAW [15] *This work	3.648	146	3.7	5.4
Sputtered AlN/Si	LWR [19]	8.53	414	0.3	1.24
Single crystalline Sc(12%)AlN/Si	LWR [16] *This work	7.96	213	5.3	11.3
Single crystalline Sc(12%)AlN/Si	LWR [16] *This work	9.02	189	4.8	9.1

Conclusion

Sputter deposition of AlN is low-cost and widely used for acoustic filter applications. However, it fails at frequencies above 2.6 GHz due to poor crystal quality of ultra-thin films. In this work, we took advantage of single-crystalline AlN epi-layers and further enhanced the piezo-response by Scandium doping. Single Crystalline AlN and Sc-AlN epi-layers can replace poly-crystalline AlN films for film thicknesses below 1 µm and show promising results for 3-10 GHz signal filtering.

Acknowledgment

The author would like to acknowledge Zhijian Hao, Mingyo park, DeaGyu Kim for the fabrication process and device measurements; and Andrew Clark and Rytis Dargis from IQE plc for the MBE growth of the epi-wafers.

References

[1] R. Vetury, "3.7GHz, Low Loss, 100MHz Bandwidth, Single Crystal, Aluminum Nitride on Silicon Carbide Substrate (AlN-on-SiC) BAW Filter." Akoustis Technologies, Inc.

[2] LTE Frequency Bands, Spectrum & Channels, [Online], https://www.electronics-notes.com/articles/connectivity/4g-lte-long-term-evolution/frequency-bands-channels-spectrum.php,.

[3] "5G Spectrum Bands," [Online], https://gsacom.com/5g-spectrum-bands/.

[4] A. Mujahid and F. L. Dickert, "Surface Acoustic Wave (SAW) for Chemical Sensing Applications of Recognition Layers," *Sensors*, vol. 17, no. 12, p. 2716, 2017.

[5] K. Tsubouchi, K. Sugai, and N. Mikoshiba, "AlN Material Constants Evaluation and SAW Properties on AlN/Al_2O_3 and AlN/Si," *1981 Ultrasonics Symposium*, 1981.

[6] M. Akiyama, T. Kamohara, K. Kano, A. Teshigahara, Y. Takeuchi, and N. Kawahara, "Enhancement of Piezoelectric Response in Scandium Aluminum Nitride Alloy Thin Films Prepared by Dual Reactive Cosputtering," *Advanced Materials*, vol. 21, no. 5, pp. 593–596, Dec. 2008.

[7] F. Martin, P. Muralt, M.-A. Dubois, and A. Pezous, "Thickness dependence of the properties of highly c-axis textured AlN thin films," Journal of Vacuum Science & Technology A 22, 361 (2004)

[8] A. Zukauskaite, G. Wingqvist, J. Palisaitis, J. Jensen, P. O. Å. Persson, R. Matloub, P. Muralt, Y. Kim, J. Birch, and L. Hultman, "Microstructure and dielectric properties of piezoelectric magnetron sputtered w-ScxAl1−xN thin films," *Journal of Applied Physics*, vol. 111, no. 9, May 2012.

[9] M. Rais-Zadeh, V. J. Gokhale, A. Ansari, M. Faucher, D. Théron, Y. Cordier, and L. Buchaillot, "Gallium Nitride as an Electromechanical Material," *Journal of Microelectromechanical Systems*, vol. 23, no. 6, pp. 1252–1271, Dec. 2014.

[10] A Ansari, VJ Gokhale, VA Thakar, J Roberts, M Rais-Zadeh, "Gallium nitride-on-silicon micromechanical overtone resonators and filters," IEEE Electron Devices Meeting (IEDM), 20.3. 1-20.3. 4 (2011).

[11] W. Wang *et al.*, "High performance AlScN thin film based surface acoustic wave devices with large electromechanical coupling coefficient," *Applied Physics Letters*, vol. 105, no. 13, Sep. 2014.

[12] www.iqep.com

[13] A. Zukauskaite, G. Wingqvist, J. Palisaitis, J. Jensen, P. O. Å. Persson, R. Matloub, P. Muralt, Y. Kim, J. Birch, and L. Hultman, "Microstructure and dielectric properties of piezoelectric magnetron sputtered w-ScxAl1−xN thin films," *Journal of Applied Physics*, vol. 111, no. 9, May 2012.

[14] J. Zou, C-M. Lin, C. S. Lam, and A. P. Pisano, "Transducer design for AlN Lamb wave resonators," *Journal of Applied Physics* 121, 154502 (2017); doi: 10.1063/1.4979914.

[15] Z. Hao *et al.*, "Single Crystalline ScAlN Surface Acoustic Wave Resonators with Large Figure of Merit (Q×kt2)"., IMS 2019.

[16] M. Park *et al.*, "A 10 GHz single crystalline Sc-AlN Lamb-wave resonator," *IEEE Transducers Conference* 2019.

[17] J. Miller, *et al.*, "Effective Quality factor Tuning Mechanisms in Microelectromechanical Devices," Appl. Phys. Rev. 5, 041307 (2018).

[18] H. Campanella, *Acoustic wave and electromechanical resonators: concept to key applications*. Boston: Artech House, 2010.

[19] High-Frequency Two-Port AlN Contour-Mode Resonators for RF Applications", Ultrasonics, Ferroelectrics and Frequency Control, IEEE Transactions on, vol.57, no.1, pp.38-45, Jan. 2010.